

**Large Scale Application Of RAPRENO_x For Emission Control In Gas
Turbines**

**Final Report
Contract Number 14-35-0001-30834**

**Robert A. Perry
Technor
1336 Concannon Blvd.
Livermore, CA 94550**

This report has been reviewed by the Minerals Management Service and approved for publication. Approval does not signify that the contents necessarily reflect the views and policies of the Service, nor does mention of trade names or commercial products constitute endorsement or recommendation for use.

This study was funded by the Minerals Management Service, U. S. Department of the Interior, Washington, D. C., under contract Number 14-35-0001-30834.

ABSTRACT

This study investigates the use of RAPRENO_x, a non-catalytic selective reduction technology, to reduce nitrogen oxides in exhaust from a 4000kW gas turbine exhaust. An exhaust system was designed and constructed in order to test the process on a full-size commercial gas turbine. The major accomplishment of this project was the successful scaling of the process to a practical system. With a simple cyanuric acid/water slurry injection system, 21 ppm NO_x was obtained in the gas turbine exhaust.

TABLE OF CONTENTS

	Page
1.0 Background	1
2.0 Experimental Work	1
2.1 General Process Description	1
2.2 Experimental Setup	2
2.2.1 Gas Turbines and Dynamometer	4
2.2.2 Duct Burner	4
2.2.3 Post Turbine Auxiliary Fuel Injection	8
2.2.4 Reactant Injection	9
2.2.5 Reaction Chamber	11
2.2.6 Reactor Design with a Water Model	12
2.3 NO _x Content	14
2.4 Exhaust Gas Analysis	14
2.5 Data Acquisition	17
3.0 EXPERIMENTAL RESULTS	18
3.1 Gas Turbine Operating Conditions	18
3.2 Reactor Operating Conditions	21
3.3 NO _x Removal with Cyanuric Acid (CYA)	23
3.3.1 NO _x Removal Data	23
3.3.2 NO _x Removal From Exhaust with Entrained Air	24
3.3.3 NO _x Removal From Exhaust without Entrained Air	25
4.0 TECHNICAL AND ECONOMIC SUMMARY FOR GAS TURBINE APPLICATIONS	28
5.0 FUTURE WORK	29
6.0 REFERENCES	30
Appendix A	32

LIST OF FIGURES

Figure 2.1 Schematic Illustrating the Function of a Recirculating Reactor	2
Figure 2.2 Schematic of the Experimental Setup, Side View and Top View	3
Figure 2.3 Schematic of Fuel Injection System.....	8
Figure 2.4 Schematic of Slurry Supply System.....	10
Figure 2.5 Schematic of Air Assisted Injector	11
Figure 2.6 Schematic of the Reaction Chamber	12
Figure 2.7 Schematic of the Water Model	13
Figure 2.8 Schematic of the Water Cooled Suction Probe.....	15
Figure 2.9 Schematic of the Experimental Gas Analysis.....	16
Figure 3.1 Experimentally Observed Exhaust Mass Flow versus Turbine Intake Temperature (TIT).....	20
Figure 3.2 NO _x Concentration Data versus CYA/NO Ratio at fixed Average Reactor Temperature of 750 C.....	23
Figure 3.3 Ratio of Initial and Final NO _x Concentration versus CYA/NO _x Ratio. (15% O ₂).....	25
Figure 3.4 Final NO _x Concentration versus CYA/NO _x ratio	26
Figure 3.5 Final NO _x Concentration versus CYA/NO _x ratio	27
Figure 3.6 Final NO _x Concentration versus CYA/NO _x ratio (Different Injection Location).....	28

LIST OF TABLES

Table 3.0 Experimental Turbine Operating Conditions	19
Table 3.1 Average Experimental Steady State Exhaust Gas Composition	21
Table 3.2 Average Experimental Conditions.....	22
Table 4.1 Estimate of Cost for Application of RAPRENOX to Gas Turbine Exhaust	30

LIST OF PHOTOGRAPHS

Photograph 2.1: Side view of the reaction chamber with intake and exhaust.....	5
Photograph 2.2: Front view of the reaction chamber with intake and exhaust	5
Photograph 2.3: Gas turbine engine mounted in test stand in front of exhaust duct	6
Photograph 2.4: Gas turbine engine with transmission about to be lifted into test cell...	6
Photograph 2.5: Test cell control room panel.....	7
Photograph 2.6: Duct burner control panel	7
Photograph 2.7: Auxiliary fuel injection system	9
Photograph 2.8: Cyanuric Acid slurry mixing system.....	11
Photograph 2.9: Gas sample probe installed in exhaust.....	17
Photograph 2.10: Data acquisition output	17
Photograph 2.11: Gas analysis station	18

1.0 BACKGROUND

The 1990 Federal Clean Air Act places strict restrictions on new sources of nitrogen oxide emissions in those areas that presently do not meet federal standards for air quality. These restrictions may impact on our nation's ability to drill for oil on offshore oil platforms where environmental concerns have already made oil exploration more difficult. The use of gas turbines on off-shore oil platforms accounts for approximately 65% of the NO_x emitted during oil exploration. Thus, a safe, cost-effective, reliable NO_x control technology for gas turbines is needed to aid in minimizing the impact of pollution control on our ability to drill for oil.

RAPRENO $_x$ promises to be suitable for this type of application. The process uses isocyanic acid, formed by the thermal decomposition of cyanuric acid, a non-toxic, nonflammable, commercially available solid material. The gaseous isocyanic acid, derived from cyanuric acid added to the exhaust stream reduces NO_x to N_2 , N_2O , H_2O and CO_2 . The fact that cyanuric acid is a solid nontoxic compound, in contrast to ammonia, makes it well suited to off-shore applications.

Another significant difference to most other post combustion selective NO_x abatement schemes that use ammonia or urea is that temperature boost and NO_x reduction are achieved simultaneously. The added fuel enhances the initiation of the NO_x reduction mechanisms by increasing the radical pool and thereby lowering the temperature requirement and the associated energy input. Recirculation decreases residence time and reactor size. Mixing of reagent and fuel occur in parallel, making elaborate injection schemes superfluous. The lean premixed combustion of the added fuel produces a negligible contribution to the overall NO_x content.

2.0 EXPERIMENTAL WORK

2.1 General Process Description

In this Process, exhaust gases, generated by gas turbines, are treated in a recirculating reactor. Fuel and cyanuric acid (CYA), the process reagent, are added to the flue gas stream before it enters the reactor. Fuel is added to increase the gas temperature to the specific effective window of reagent, and to enhance the NO reduction chemistry. CYA is a solid and is injected as water-based slurry. The process reagent and the added fuel trigger a chain reaction that selectively reduces NO_x .

Operating temperatures in the recirculating reactor are controlled between 700 and 750°C. This temperature range is based on results of previous work showing significant NO_x reduction in Diesel engine exhaust in the presence of hydrocarbon radicals at an operating range of 680-760°C [Perry, 1991] [Streichsbier, 1998].

Since exhaust gases from a turbine reach a maximum temperature of approximately 600°C, heating of the exhaust gases becomes necessary. The temperature boost is achieved by

autoignition of the additionally injected turbine fuel in the reactor's recirculating zone. Recirculation provides mixing of hot combustion products with the incoming cooler, less reactive, stream. The subsequent temperature rise combined with the increased concentration of radicals triggers the combustion of the mixture to so establish a stable reaction zone.

This principle is the basis of many flame holding techniques, (e.g. the afterburner in a jet airplane engine) especially in fuel lean ($\Phi < 1$) combustion scenarios. (The process here is considered as very lean with equivalence ratios below $\Phi = 0.05$).

In contrast to typical flame holders, recirculation is brought about not by insertion of blunt bodies, partially blocking the flow, but by changing the direction of the gas flow velocity in the chamber. (See Figure 2.1.)

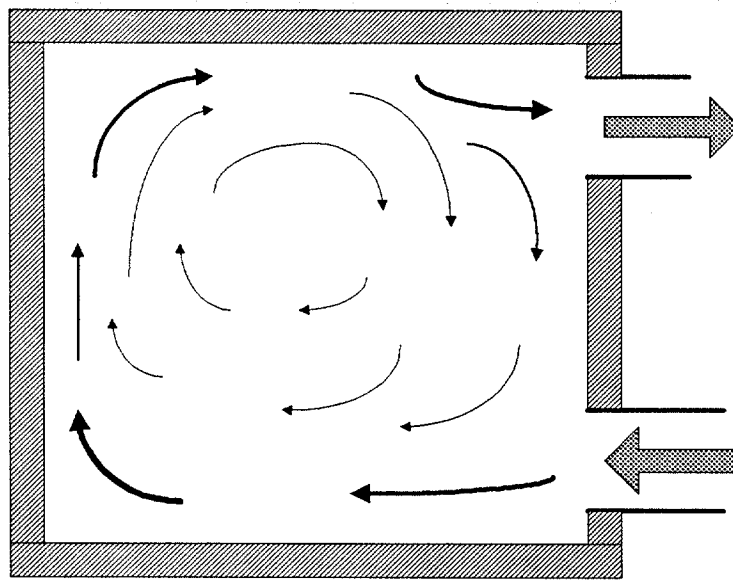


Figure 2.1: *Schematic Illustrating the Function of a Recirculating Reactor*

The significant difference to most other NO_x abatement schemes is that temperature boost and NO reduction are achieved simultaneously. The added fuel enhances the initiation of the NO_x reduction mechanisms by increasing the radical pool and thereby lowering the temperature requirement and the associated energy input. Recirculation decreases residence time and reactor size. Mixing of reagent and fuel occur in parallel, making elaborate injection schemes superfluous. The lean premixed combustion of the added fuel produces a negligible contribution to the overall NO_x content.

2.2 Experimental Setup

All experiments were performed in conjunction with National Airmotive Corporation (NAC). Note that NAC was purchased by Rolls Royce (RR) during the testing. The testing facility (NAC/RR) in Oakland, California overhauls and tests oil and gas burning gas turbines of up to 5 MW. Gas turbine and attached water brake dynamometer are located in a test cell. The exhaust

gas treatment reactor and all associated accessories are fitted to the cell, replacing the normally used exhaust stack. Figure 2.2 shows a schematic of the duct and the reactor that replace the

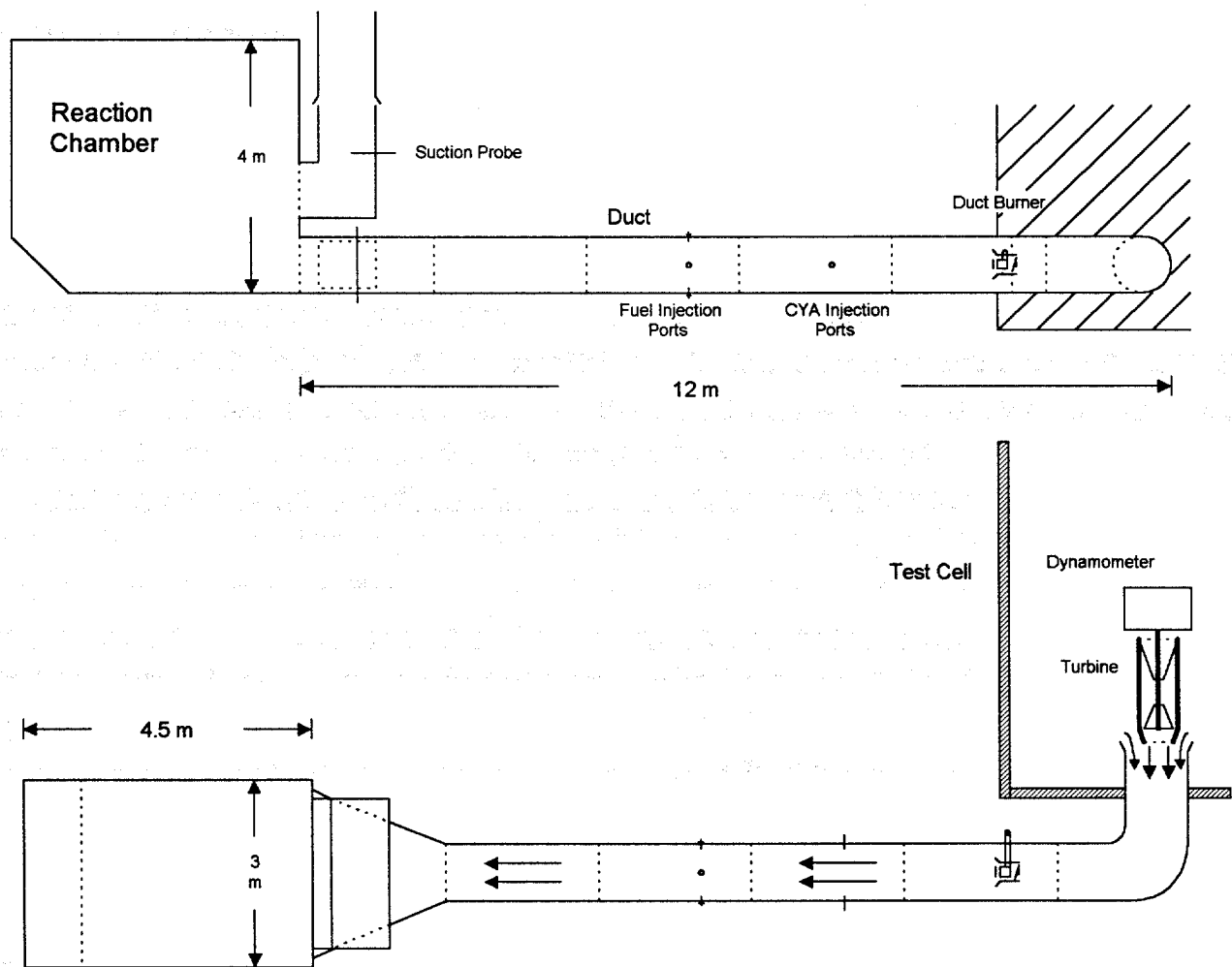


Figure 2.2: *Schematic of the Experimental Setup, Side View and Top View.*

exhaust stack. Gas turbine and dynamometer are controlled and monitored from a separate control room. The exhaust gases produced by the turbine are ducted out of the test cell entraining test cell air. This entrained air maintains a specified cell depression and cools the exhaust flow. Entrainment varies between 20 and 50% depending on the shape of the turbine, engine speed and applied load. At full load the maximum mass flow through the duct reaches as much as 26 kg/s. A duct burner boosts the exhaust gas / cell air mixture to simulate turbine exhaust gas temperature and is also used to raise this temperature closer to the reactor temperature. Both process reagent, CYA, and the additional fuel are injected directly into the exhaust gas stream down stream from the duct burner and mixed in the highly turbulent flow prior to entering the reactor.

The duct is internally insulated and has an inner diameter of 92 cm and a length of 12 m. At a mass flow between 20 and 26 kg/s and a temperature of 600°C the exhaust gas flow becomes

highly turbulent reaching speeds 40 m/s. A 2.4 m transition section connects the duct to the exhaust gas treatment reactor, spreads the flow and thereby reduces the flow velocity. Photographs 2.1 and 2.2 show the actual experimental setup.

2.2.1 Gas Turbines and Dynamometer

A gas turbine engine is a heat engine consisting of a compressor, a combustion chamber and a turbine. Intake air is compressed and fuel is injected into the compressed flow. The so obtained fuel – air stream is then ignited and combusts, resulting in a stable non-premixed overall lean burning combustion process. Following combustion these hot compressed gases enter the turbine nozzle and expand through the turbine wheels where power is extracted to drive compressor, engine accessories and provide output shaft power.

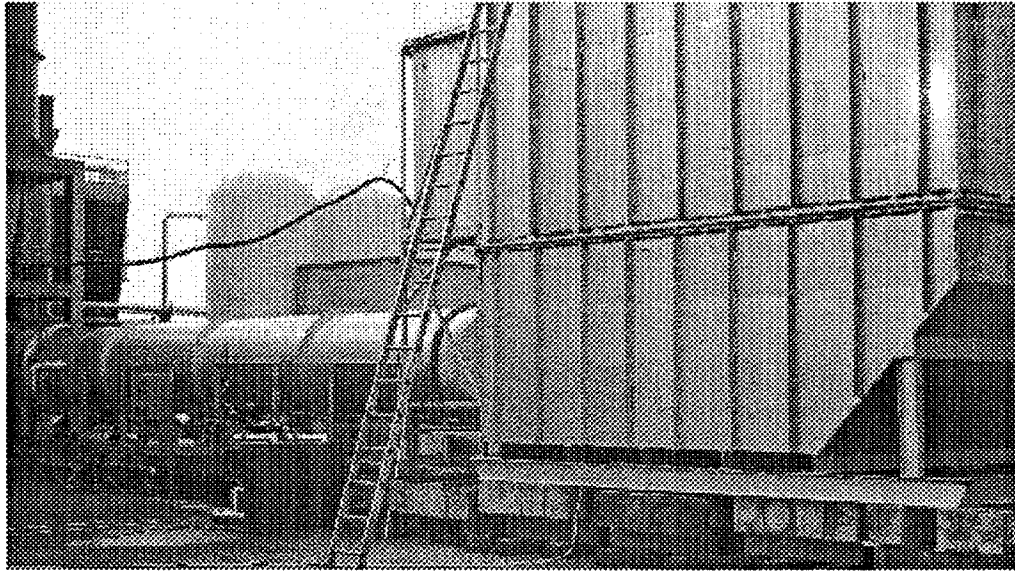
In these test we used an Allison K501 industrial style gas turbines and flight engines with a rated maximum output of up to 4200 kW. Their speeds are governed to approximately 10000 rpm (680 s^{-1}). A planetary transmission reduces output shaft speed to 1000 rpm (100 s^{-1}) and links the engine output to a water brake dynamometer, which provides a controllable load up to 10000 kW.

Engine and dynamometer are both aligned and rigidly mounted to the test cell floor. The water brake dynamometer transforms mechanical energy into heat via viscous dissipation. The entire test stand has been provided by Froude Engineering. Photographs 2.3, 2.4 and 2.5 show turbine engine test stand and control equipment.

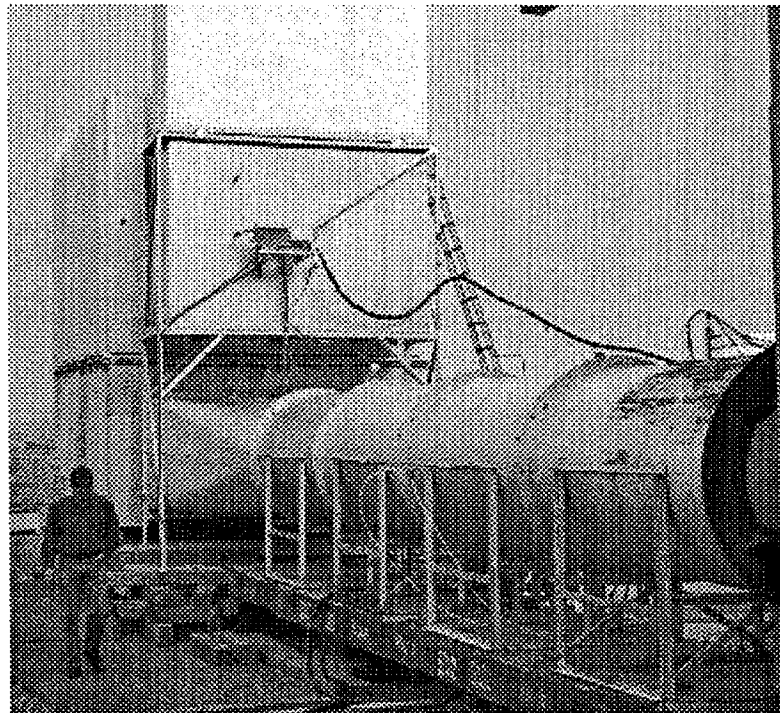
All turbine engine data relevant to integrity and performance of the engine, such as air intake, compressor and turbine exit temperatures as well as fuel consumption are continuously monitored. Typical Engine data are provided in the Appendix A. A typical test schedule includes engine operation at low medium and high loads. Load following and speed control are achieved in the turbine engine by varying fuel injection pressure and corresponding fuel input.

2.2.2 Duct Burner

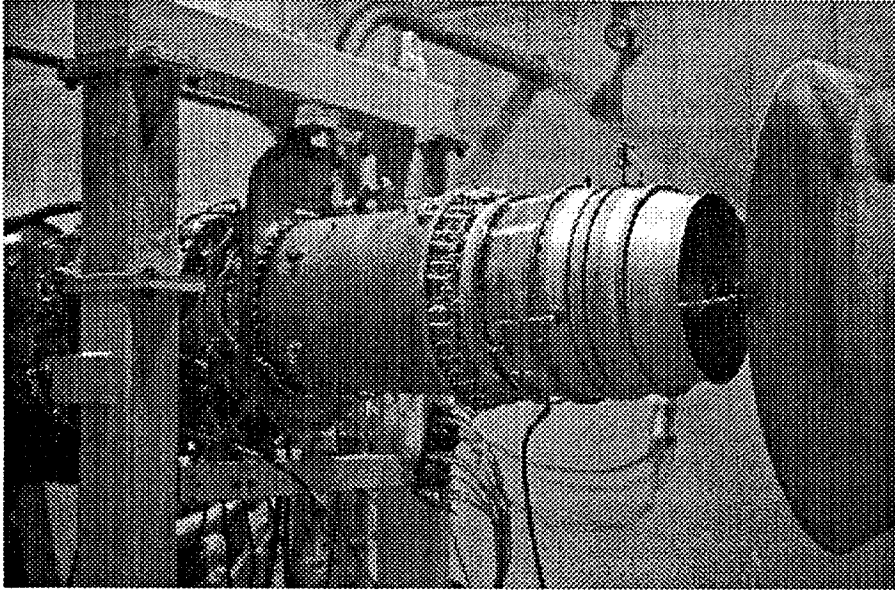
In normal operation mode the exhaust gases coming from the turbine are diluted with entrained “cold” test cell air. A duct burner is used to achieve exhaust gas composition and an elevated temperature corresponding to a gas turbine exhaust produced under high load conditions. The duct burner is an independent unit and operates on simulated natural gas. It is installed in the exhaust duct approximately 5 m downstream of the turbine nozzle and adds a maximum of 1000 Pa (~ 4 in of water) to the overall pressure drop across the entire system. The burner consists of a donut shaped fuel injection body, swirling vanes and a pilot flame for ignition. A throttle plate-metering valve controls the exhaust / air flow through the injection body. A second metering valve connected to the throttle plate valve controls the fuel flow. A single servomotor governs both valves. By coupling air flow to fuel flow an overall equivalence ratio can be maintained. A PID controller drives the servomotor using a thermocouple in the duct down stream, a user supplied set point temperature and a flame sensor as inputs. Photograph 2.6 shows the duct burner control panel.



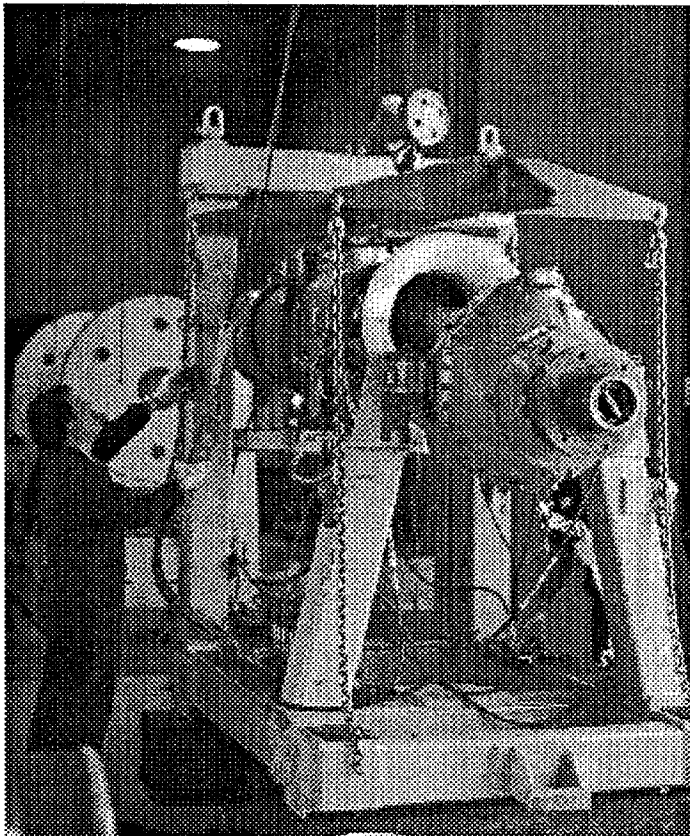
Photograph 2.1: Side view of the reaction chamber with intake and exhaust.



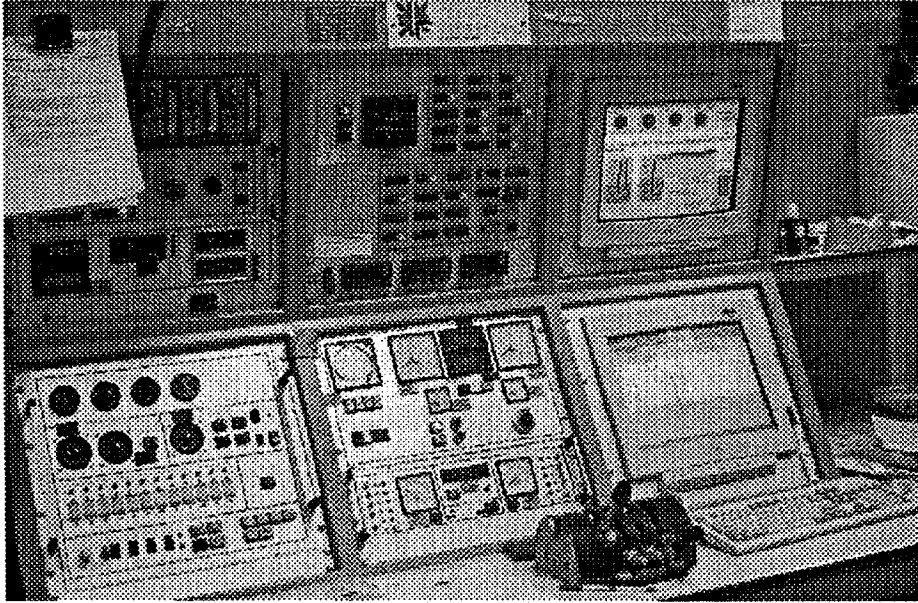
Photograph 2.2: Front view of the reaction chamber with intake and exhaust.



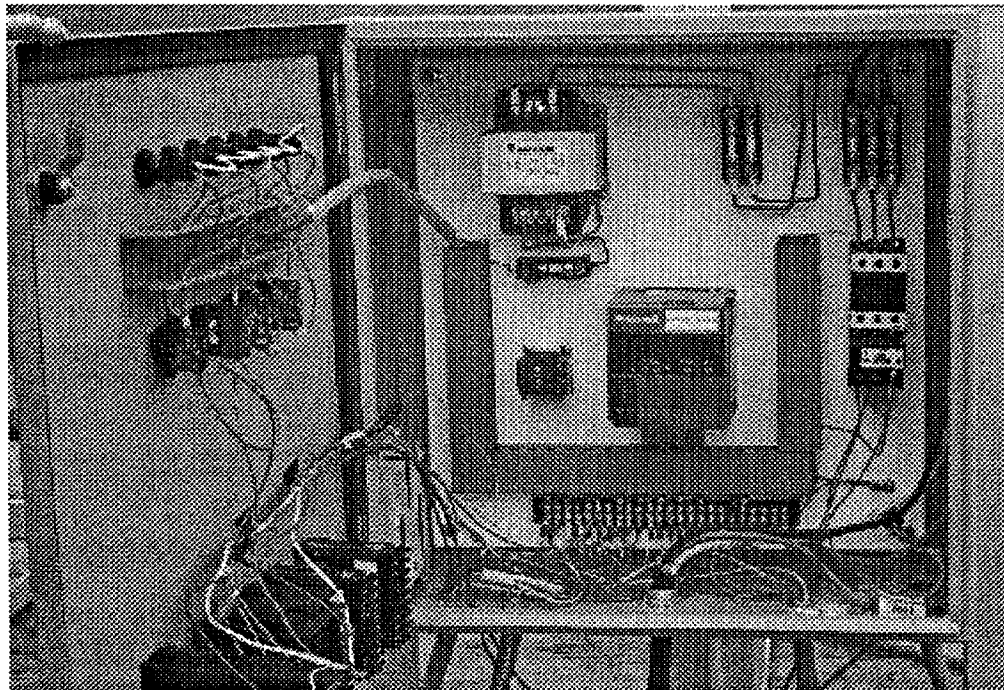
Photograph 2.3: Gas turbine engine mounted in test stand in front of exhaust duct



Photograph 2.4: Gas turbine engine with transmission about to be lifted into test cell



Photograph 2.5: Test cell control room panel.



Photograph 2.6: Duct burner control panel.

2.2.3 Post Turbine Auxiliary Fuel Injection

To allow operation at a fixed reactor temperature and provide the hydrocarbon radical pool, necessary to enhance the NO_x reduction chemistry, a controlled amount of auxiliary fuel is injected into the exhaust gas stream. This jet fuel injection occurs 5 m downstream of the duct burner. To achieve proper mixing four calibrated stainless steel injector nozzle are mounted pointing into the center of the exhaust duct opposing each other. A multiple chamber gear pump supplies fuel pressure. A control unit, receiving its signal from a PID controller coupled to the reactor temperature drives a relief valve controlling the fuel flow returning to the jet fuel tank.

Changing the return fuel flow rate changes the supply pressure to the nozzles and there by the amount injected. The fuel flow is monitored with a liquid flow meter. Solenoid valves provide emergency shut off. The injection nozzles produce a 90-degree cone when fluid is expelled into a still body of air. A schematic of this system is provided in Figure 2.3. The actual system is depicted in Photograph 2.7.

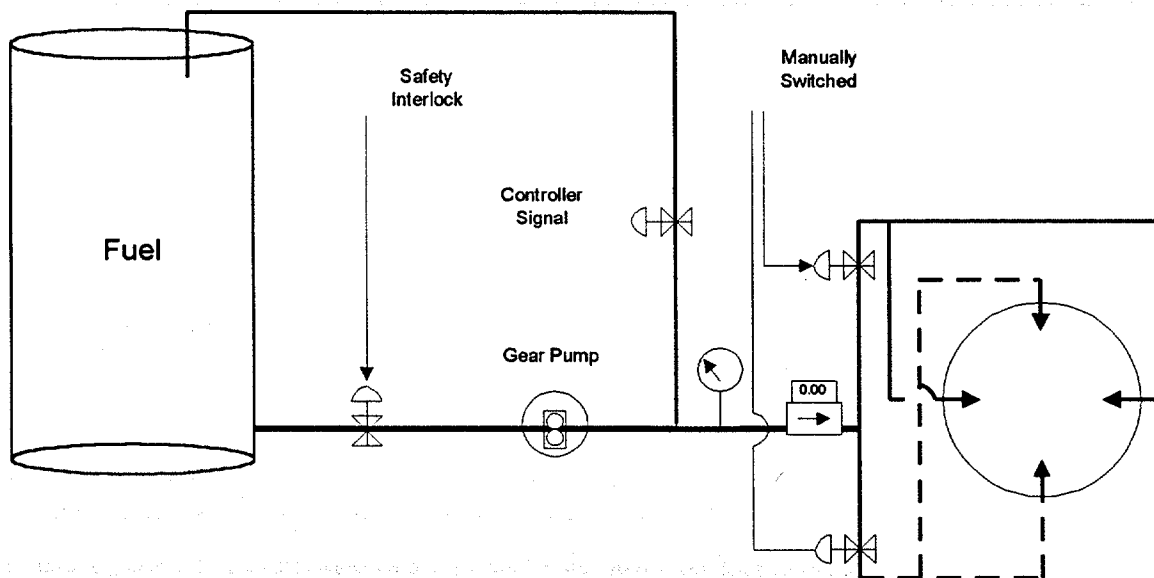
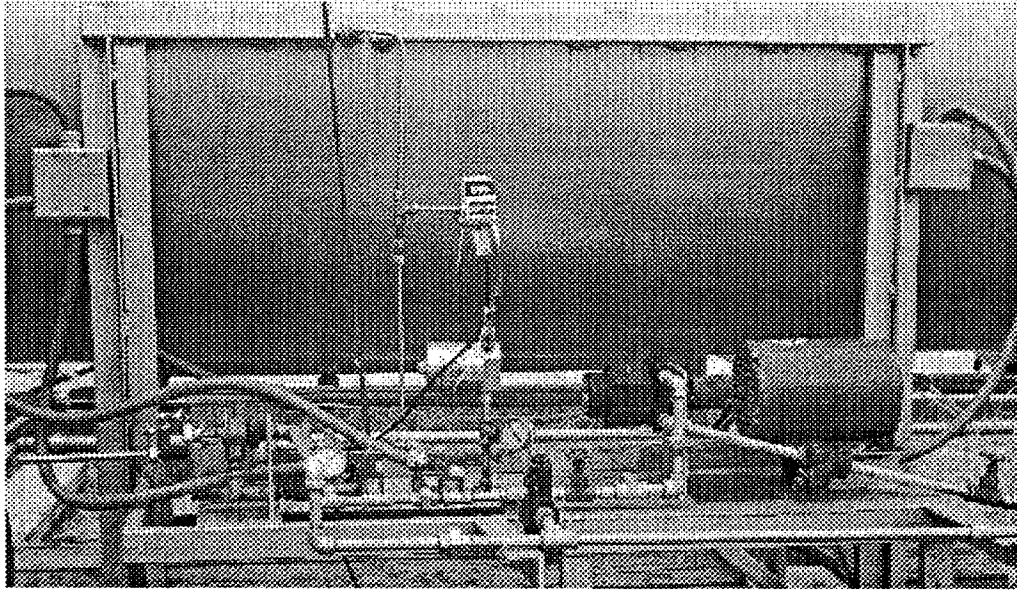


Figure 2.3: Schematic of the Fuel Injection System



Photograph 2.7: Auxiliary fuel injection system.

2.2.4 Reactant Injection

Mixing of exhaust gases with the proper amount of cyanuric acid (CYA) is crucial to the NO_x removal efficiency. It is therefore important to be able to continuously meter and control the quantity of CYA that is injected. In this project, CYA is injected as water slurry. Using an incompressible fluid, such as water, as carrier, facilitates reliable CYA injection over a wide range of feed rates. Automated control mechanisms are employed to allow load following and NO_x content based variation of these injection rates. In order to benefit from turbulent mixing CYA is introduced in as far upstream from the reactor as possible.

Prior to the gas phase NO reduction the injected reagent has to sublime and decompose from CYA, $(\text{HNCO})_3$, to isocyanic acid (HNCO). This occurs at temperatures above 330°C . Any injection system therefore has to be able to withstand exhaust gas temperatures and to deliver a spray of particles that are small enough to sublime in the hot coflow before entering the reaction zone.

Cyanuric acid is a nontoxic white infusible crystalline solid and only moderately soluble in water. Since earlier efforts have shown that dry powder injection is troubled with injector clogging and does not appear to be practical in an industrial application, a different mode of injection, using water as a carrier, has been chosen.

To insure a homogeneous distribution of the suspended particles in the water, i.e. from a slurry, the suspension has to be continuously agitated. This is done by a pump circulating the mixture, at a rate of approximately 100 l/min, from the bottom to the top of a 200-liter storage container. See Figure 2.4 and Photograph 2.8 for the entire injection system.

A Bailey SLC 1 controller operates a peristaltic pump to deliver the desired amount of slurry through two 9 mm inner diameter tubes from the holding container to the injectors. NO_x concentration and reagent/water ratio are manually input into the controller. Tubing, carrying the slurry to the injectors, is sized such that the flow velocity prohibits settling out of the reagent powder.

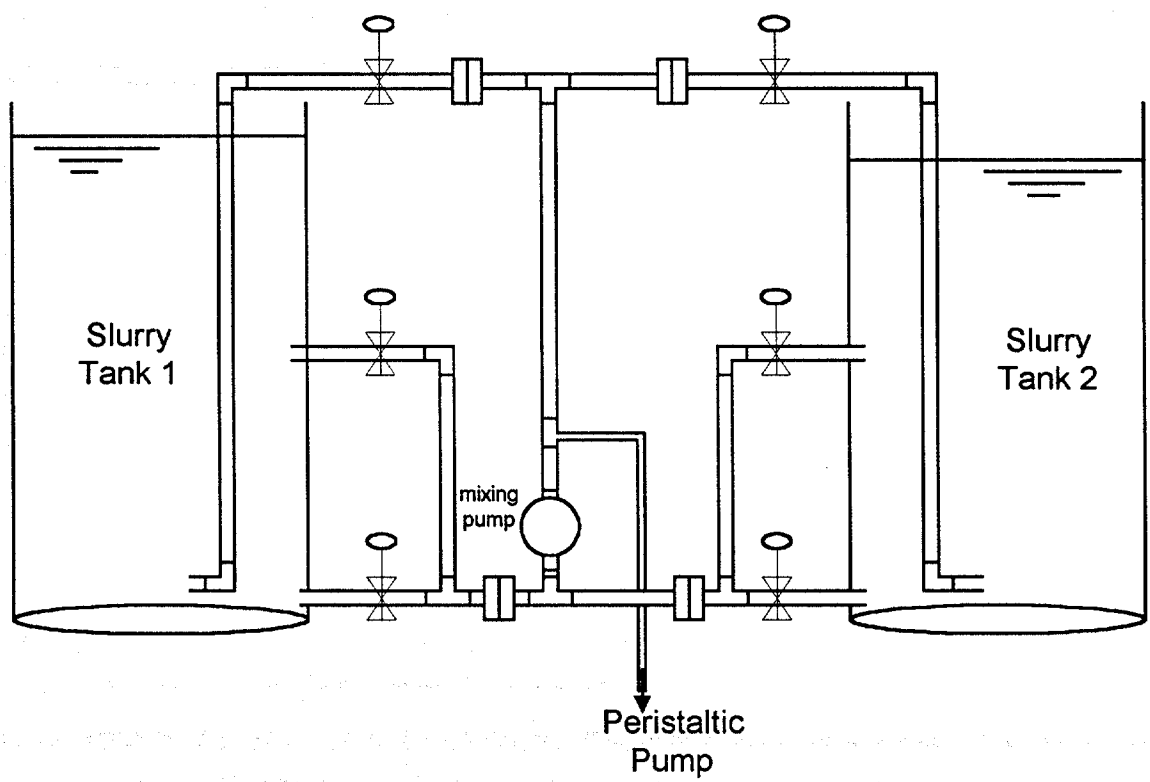


Figure 2.4: *Schematic of the Slurry Supply System*

The two injection systems that have been built use compressed air assisted coaxial injectors. See Figure 2.5. They allow injection of various amounts of slurry of different consistency into the hot turbine exhaust stream. Droplet size was found to be dependent on compressed air flow. Pressure drops across the injectors are negligible at given slurry flow rates. Injection occurs perpendicular to the flue gas flow 6 m upstream of the reaction chamber. The injectors are fitted through access ports in the duct to oppose each other and can be inserted to various depths.

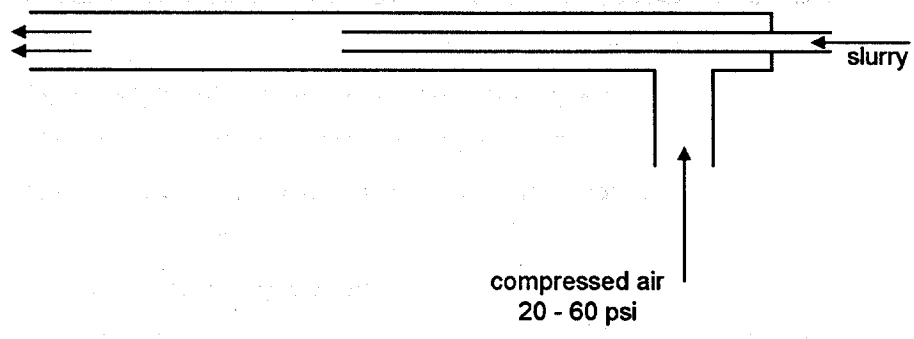
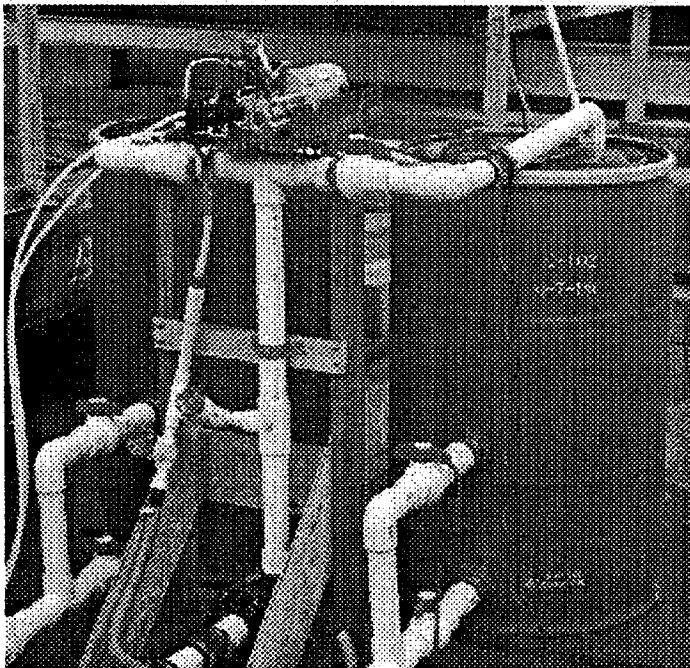


Figure 2.5: *Schematic of Air Assisted Injector*



Photograph 2.8: Cyanuric acid slurry mixing system.

2.2.5 Reaction Chamber

In the design of the reaction chamber the following constraints were considered:

- 1) The reaction chamber has to be large enough to allow sufficient residence time for autoignition of the added fuel and NO removal;
- 2) Reactor geometry has to induce recirculation of the incoming flow;
- 3) The exhaust gases have to be guided through the reactor without significant pressure loss;
- 4) The chamber has to be chemically inert, i.e. catalytic surfaces have to be minimized by keeping the surface to volume ratio low; and
- 5) The reactor has to remain structurally intact at elevated temperature to reduce loss of heat .

These requirements are best met with a rectangular design. The final reactor geometry was determined using a water model as outlined in Section 2.2.6.

The actual reactor is assembled out of 2 welded prefabricated units bolted together in place. These pre-fabricated segments are easily transported to the site location. Ribs of 1.3 by 10 cm flat steel provide structural strength to the welded 6.25 mm steel reactor shell. The reactor is internally insulated with 15 cm rigid insulation. The insulation can withstand 2000 K with a total thermal conductivity rating of $k = 0.5 \text{ W/K}\cdot\text{m}^2$. The overall volume of the reactor is 58 cubic meter, which translates to a minimum residence time of about 0.75 seconds at maximum exhaust mass flow and a temperature of 750°C.

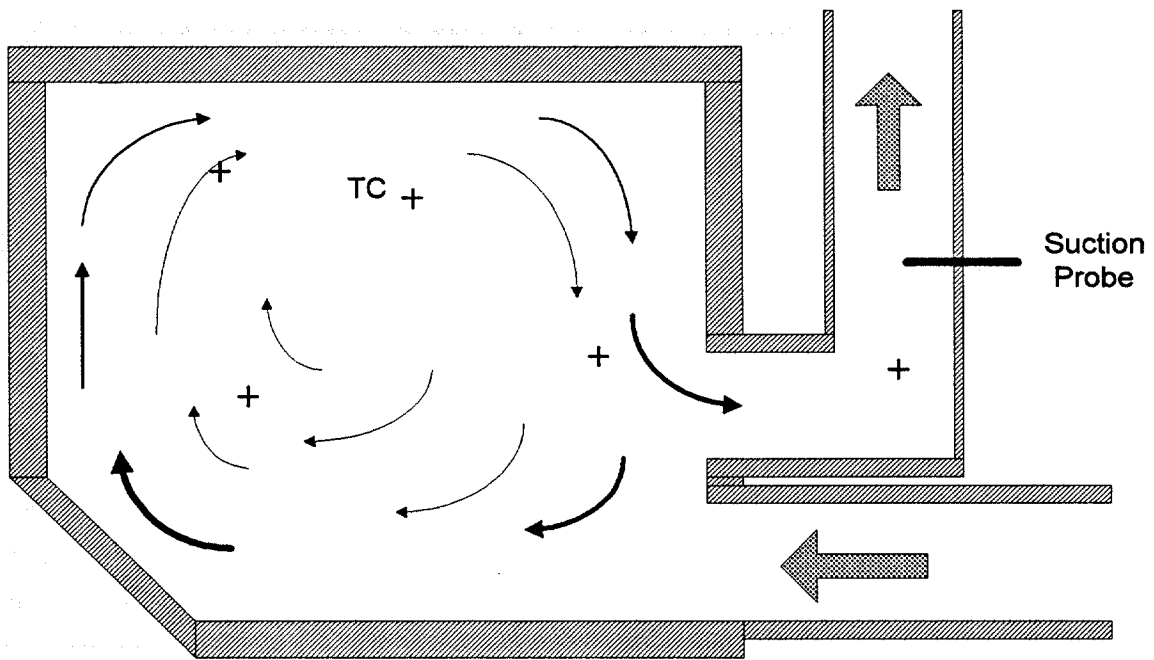


Figure 2.6 *Schematic of the Reaction Chamber*

All surfaces have been coated with a ceramic insulation rigidizer and sealant to minimize erosion and catalytic interactions. A door provides access to the chamber. Thermocouples are inserted through the insulated walls. A pressure tab and a water-cooled suction probe for exhaust gas analysis are located in the exhaust section of the reactor.

2.2.6 Reactor Design with a Water Model

A water model has been used to optimize recirculation and mixing and to reduce the associated pressure drop across the reactor to below 500 Pa (2 inches of water). Since any back pressure applied to the exhaust of the gas turbine constitutes a parasitic load, the necessary recirculation to achieve the exchange of heat (and radicals) from the reacting to the incoming stream, should be induced with minimum pressure loss. Typically used geometries such as bluff bodies immersed into the flow have large area blockage which leads to high pressure losses [Lovett et al., 1995]. The idea here is to force the incoming flow into recirculation without submersion of a high drag object or reduction of the effective cross sectional area. An expansion combined with a change of the direction of the fluid velocity is used. To optimize the proposed reaction chamber geometry,

a water model was built to the scale of 1:12. It contained two adjustable wings to direct the flow and allowed modifications of all partition lengths and locations.

The plexiglass model was submerged in a water tank to reduce optical distortion and circumvent the potential problem of leakage and air entrainment (see Figure 2.7). The conditions of similarity were fulfilled geometrically by properly scaling each relevant length 1:12. This particular size was chosen to keep the water throughput manageable.

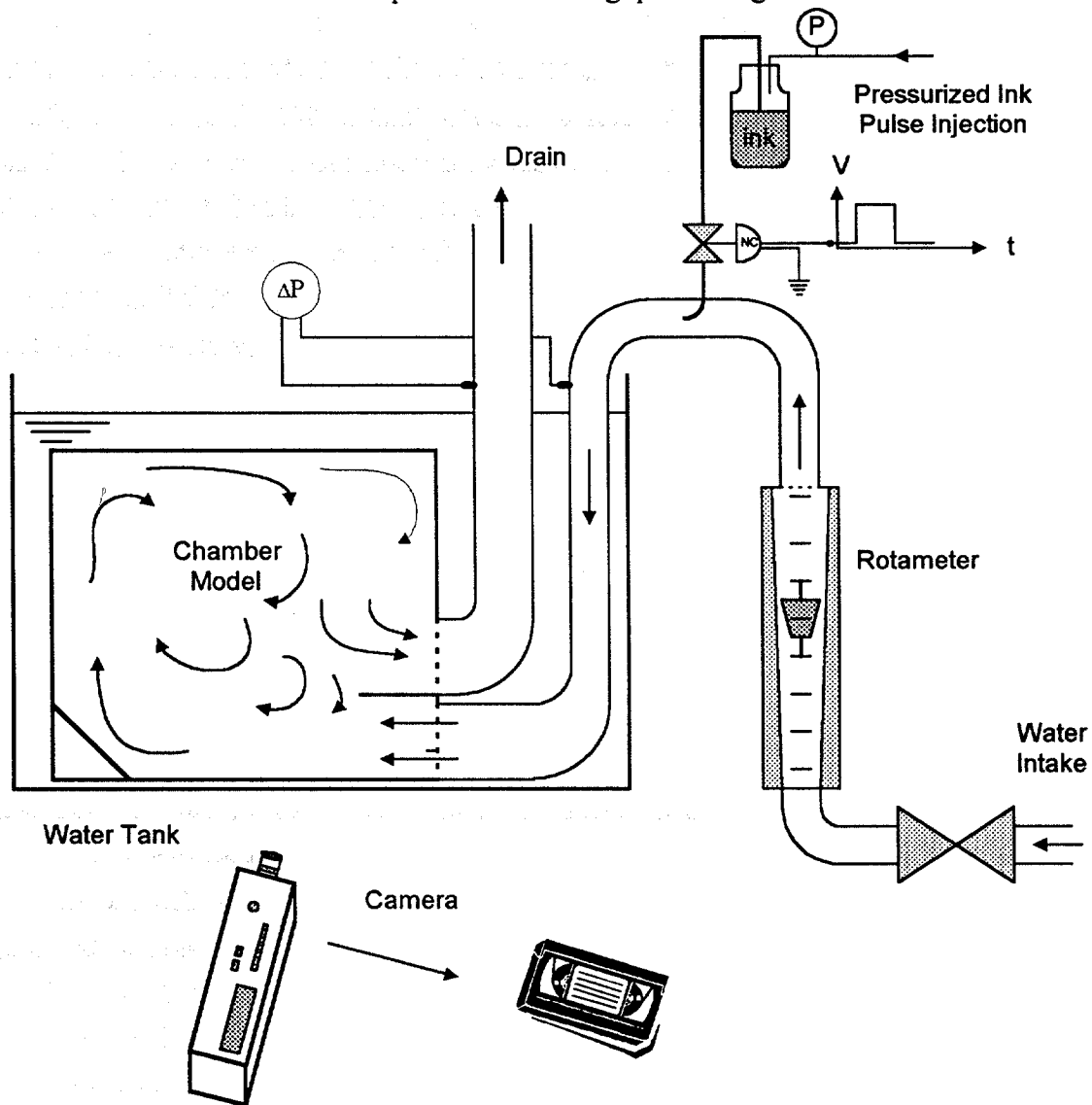


Figure 2.7: *Schematic of the Water Model*

The Reynolds number at the intake was kept similar ($Re > 50000$) throughout the experiment. Mass flow was determined with a rotameter. Since the chosen fluid has different properties than exhaust gases, Peclet number similarity could not be obtained as long as Reynolds number similarity exists. In this case turbulent transport phenomena were assumed to be dominant and the Peclet number difference was ignored [Rhine, 1991]. Density variations within the fluid were also neglected.

A function generator applied a single step of 0.5 second duration to a solenoid valve. The valve opened and delivered ink, kept at a constant pressure, with a pulse of known width. The subsequently visible flow pattern was observed with a video camera (25 frames/s). Recirculation ratio and mixing quality were estimated by opacity comparison, frame by frame, for various reactor geometries. The pressure drop across the reactor was obtained with a manometer as indicated in Figure 2.7.

These qualitative assessments led to the gas phase reactor shown in Figure 2.6. The incoming flow is directed upward with a 45 degree partially inclined back wall. The estimated recirculation ratio is approximately 30% at an average residence time $\tau = 0.75$ s. The overall pressure drop across the exhaust gas treatment reactor is 500 Pa (2 inches of water).

2.3 NO_x Content

The turbines used in this project produce NO_x emissions of 80 to 160 ppm (at 15% O₂) at full load, depending on whether they are operated on gaseous or liquid fuel respectively. Entraining test cell air can lower the measured initial NO_x concentration by as much as 50% in the exhaust gas stream. Tracking fuel consumption and CO₂ concentration in the diluted exhaust allows the calculation of the amount of entrained air and thereby the total amount of NO_x emitted.

Once the duct burner is turned on and the auxiliary fuel injected, additional NO_x is generated boosting the net NO_x concentration in the exhaust inside the reactor chamber at the experimental conditions sampled. Due to the consumption of oxygen by the burner the NO_x concentration adjusted to 15% O₂ declines compared to NO_x concentrations due only to the turbine when adjusted to 15% O₂.

2.4 Exhaust Gas Analysis

Exhaust gases are sampled continuously. A water cooled suction probe is located downstream of the reaction chamber. A sample pump, with attached filter, provides 0.3 bar of exhaust sample pressure to an analysis station. Suction probe, pump, filter and connecting teflon line are heated above the dew point of water (~ 70°C). A refrigerator sample dryer and a gas phase "Nafion" membrane sample dryer which remove selectively water vapor ensure that all measurements are taken on a dry gas basis. Gas composition analysis is performed by a set of instruments consisting of:

- A **TeCo Chemiluminescent NO / NO_x** analyzer. NO reacts with O₃ to form excited NO₂ and O₂. Photons emitted from the excited NO₂ are detected by cooled photo multiplier tube. The photo multiplier output signal is proportional to the NO concentration.
- A **Horiba Infrared CO** and a **Horiba Infrared CO₂** analyzer. Molecules of CO and CO₂ absorb infrared light at specific wavelengths. The absorption is proportional to the concentration of the molecule.

- A **Teledyne Fuel Cell O₂** analyzer. A current is generated inside a fuel cell when exposed to O₂. The measured current is proportional to the O₂ concentration.

The analyzers are calibrated directly before experiments using certified calibration gases with concentrations of approximately 80 – 90% of the working range. Drawing 2.9 shows a schematic of the gas analysis station. Photographs 2.9 and 2.11 show sampling system and the gas analysis instrumentation.

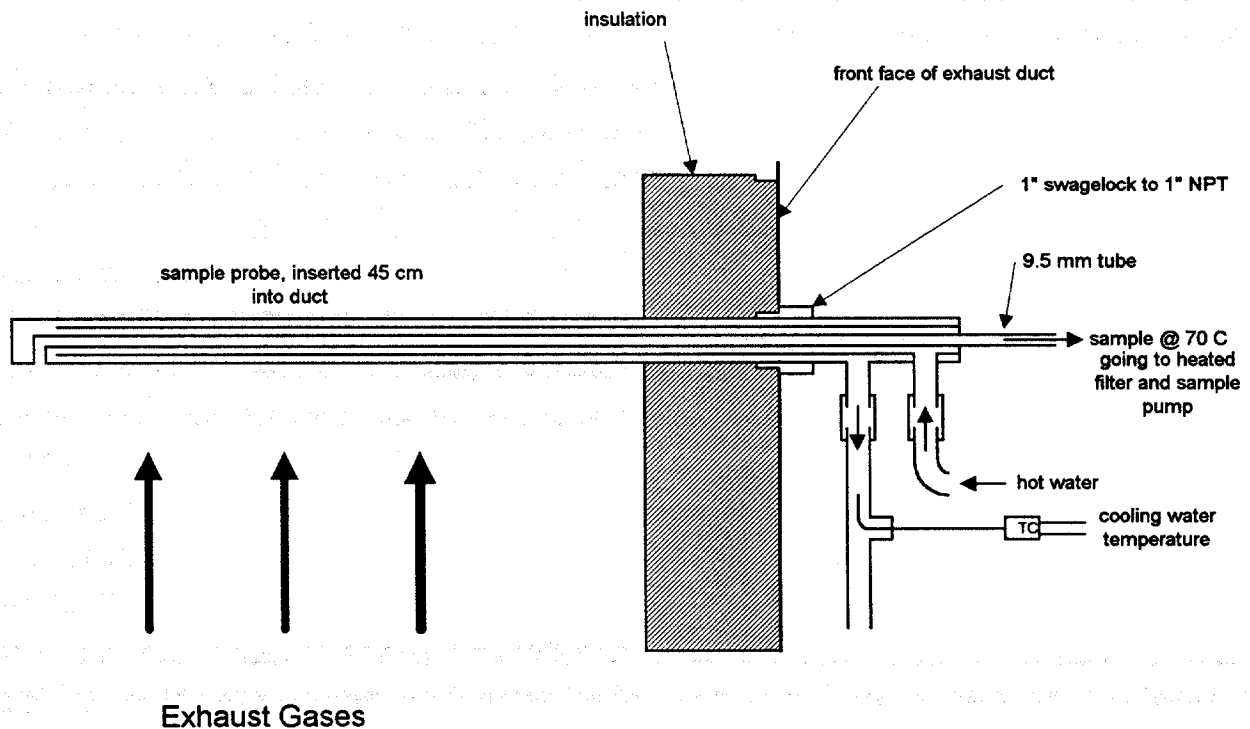


Figure 2.8 *Schematic of the Water Cooled Suction Probe*

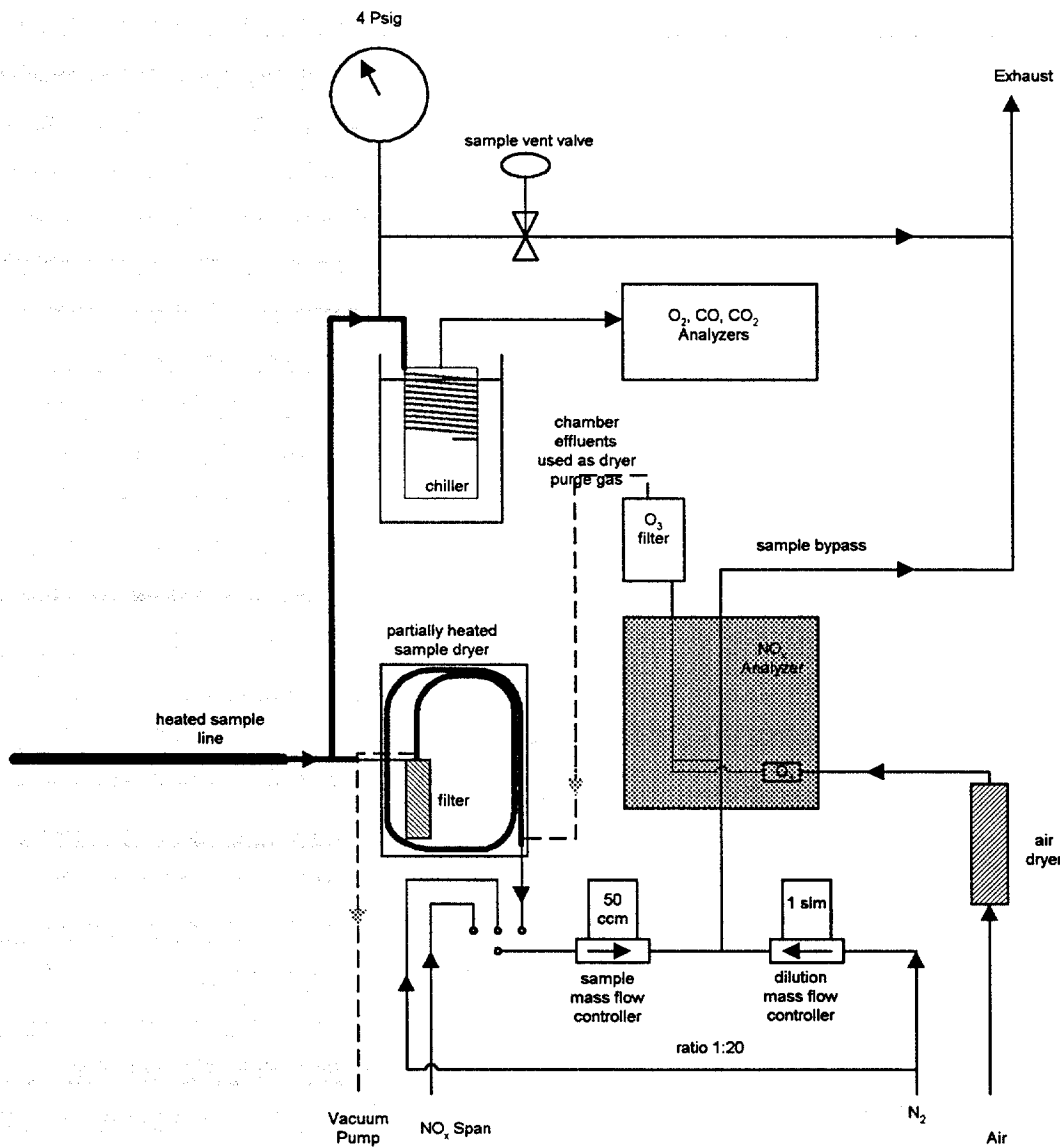
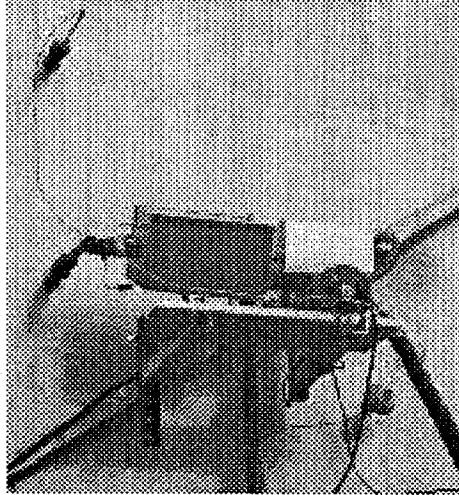


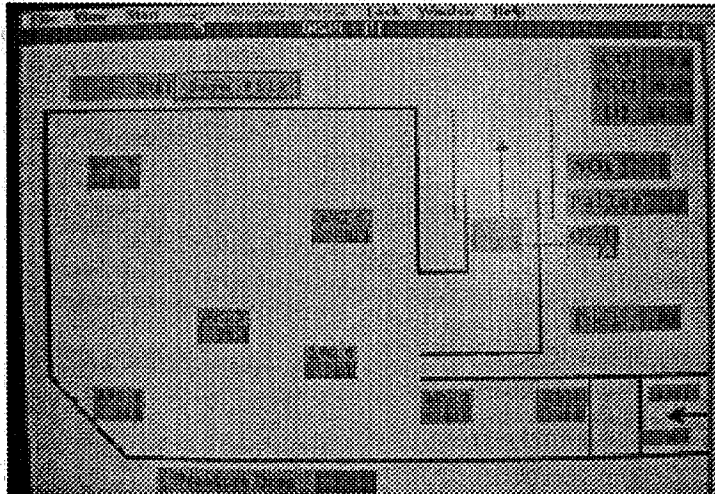
Figure 2.9: Schematic of the Experimental Gas Analysis



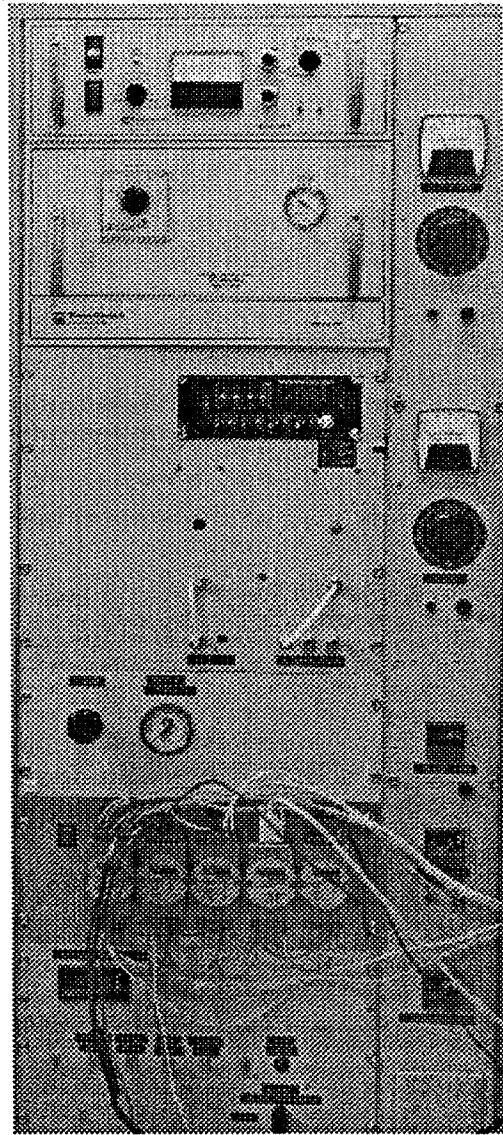
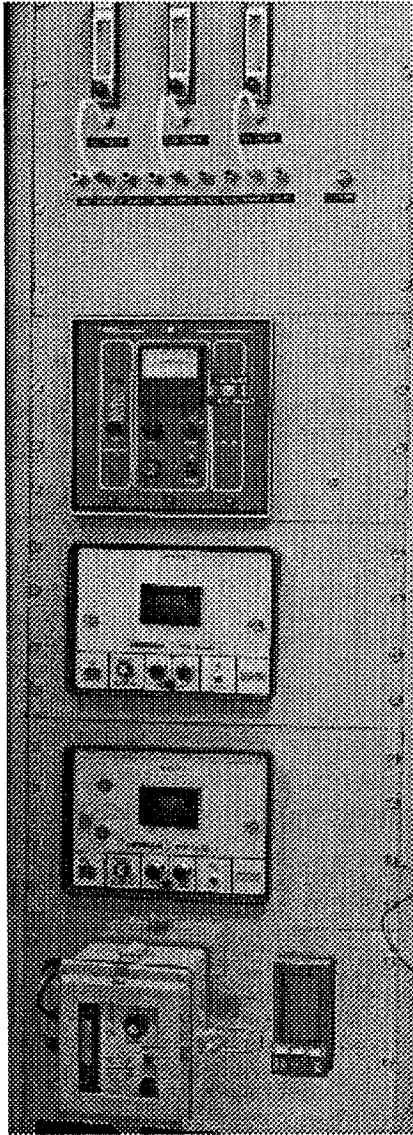
Photograph 2.9: Gas sample probe installed in exhaust.

2.5 Data Acquisition

All temperature, pressure, fuel flow and gas composition data were collected at a 1Hz frequency. Adam modules processed the incoming data remotely. The modules communicated with a PC through an RS 232 serial port. All information was displayed on screen, shown in Photograph 2.10, and written to file during the experiments.



Photograph 2.10: Data acquisition output.



Photograph 2.11: Gas analysis station.

3.0 EXPERIMENTAL RESULTS

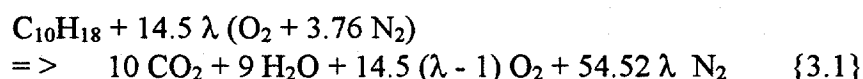
3.1 Gas Turbine Operating Conditions

The turbines tested at the NAC/RR facility were found to operate with the attached duct and exhaust gas treatment reactor as reliably as with the replaced exhaust duct. The backpressure of duct, duct burner and reactor combined reached a maximum of 1800 Pa (~ 7 inches of H₂O) at maximum reactor temperature. During a typical test cycle turbines were loaded in incremental steps to reach maximum output of approximately 3.5 MW (~ 4800 hp). There were two operating modes:

- A. The turbines were mounted such, that air is entrained into the exhaust duct with the exhaust gases leaving the turbine nozzle. Consequently, the resultant exhaust mass flow consisting of turbine exhaust and test cell air was larger than the mass flow through the turbine. This was the regular mode of operation.
- B. The flow of cell air to the exhaust duct was blocked off such that only turbine exhaust entered the exhaust gas treatment reactor.

Direct flow measurements of the large exhaust mass flow, encountered in either mode, are impractical and difficult, especially considering the backpressure requirement. Nevertheless, exhaust mass flow was determined using a stoichiometric balance based on the fuel mass flow, obtained from a calibrated mass flow meter, the fuel composition and the CO₂ or O₂ concentration in the exhaust. The composition of the used Jet fuel (Jet A1, JP-4) was assumed to be C₁₀H₁₈ [Turns, 1996]

In the overall equation:



the factor λ ($\lambda = 1/\Phi$) can be obtained independently via either CO₂ or O₂ concentration measurements. Note that under the first operating condition (A), λ is larger since the entrained air is included into the total air flow in equation 3.1. In either mode both values of λ , based on CO₂ or O₂ measurements, were found to agree with each other within the limits of experimental uncertainty. Because of these two modes of operation, exhaust mass flow and the respective experimental results are not immediately comparable and are listed separately.

Table 3.0 shows some of the experimental turbine operating conditions at high applied loads. The listed turbine exit temperature is the temperature of the exhaust gases leaving the turbine. When no air is entrained this is approximately the temperature of the exhaust gases in the duct. When air is entrained it cools the exhaust mass flow and lowers the duct temperature by as much as 150°C.

m _{fuel}		λ	m _{air}	Temperature	Load	Efficiency	Exhaust Gas Composition (dry)			
(kg/min)	kW						(kg/s)	turbine exit (C)	kW	%
15.32	11670	2.86	13.900	490.0	2596	22.2	3.78	15.05	83.0	63
15.59	11874	3.02	14.900	526.0	2700	22.7	4.02	15.45	95.2	80
16.40*	12490	3.74	15.040	522.0	2898	23.2	3.56	14.9	93.4	195

Table 3.0: *Experimental Turbine Operating Conditions. Note that a value of $\lambda > 1$ corresponds to fuel lean conditions. (* liquid fuel equivalent, since engine was run with propane)*

Although most of the tested turbine engines were similar in size and mass flow, turbine nozzle geometry and test procedure can change the amount of entrained air. The total exhaust mass flow through the treatment reactor obtained by the above-described method can be seen in Figure 3.1. The resulting values carry a 2 - 3% uncertainty. Intake air pressure and humidity was not determined and did not enter this calculation. Some of the observed variations are therefore a consequence of changes in barometric pressure and the ambient level of humidity. While the T56 style engines consistently produced an exhaust mass flow of 25.2 to 26.5 kg/s, exhaust mass flows of KB 501 engines showed

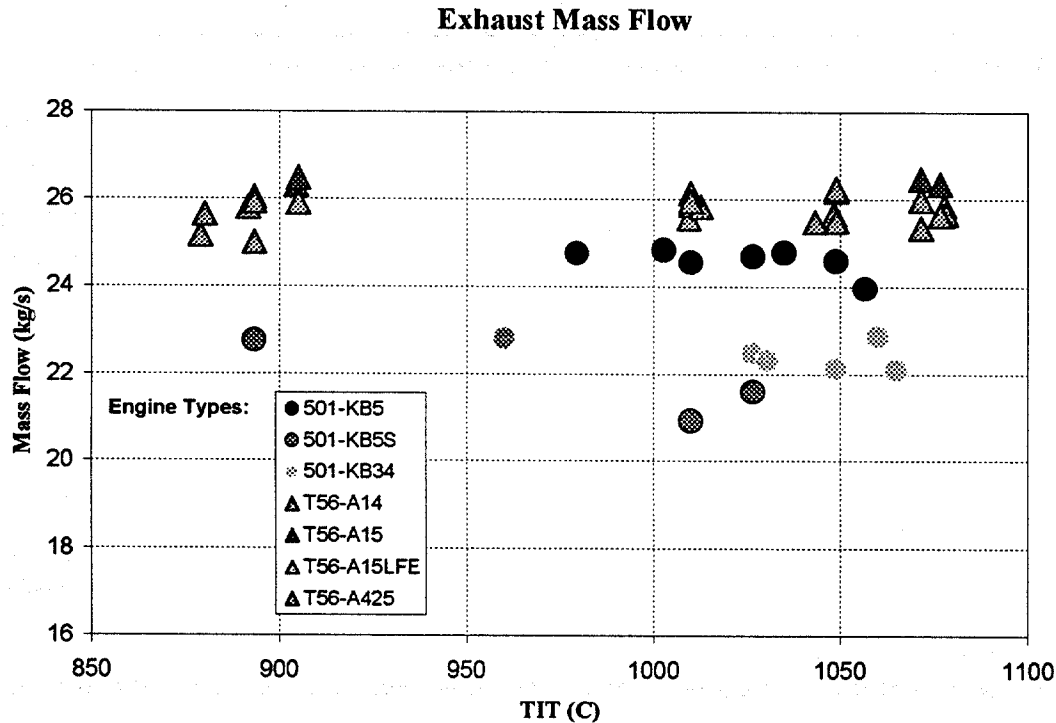


Figure 3.1: Experimentally Observed Exhaust Mass Flow versus Turbine Intake Temperature (TIT). The TIT depends on fuel input and turbine speed and is thus indicative of turbine load.

more variation, 20.9 to 24.9 kg/s, and lower overall values. During each test exhaust mass flow appeared to be largely independent of the applied load in the tested load regime. Fuel flow at maximum load varied between $\dot{m}_{fuel} = 16.8$ to 18.7 kg/min. At a lower heating value of 45.5 MJ/kg for Jet A-1 fuel the total energy input ranged between 12.8 and 14.3 MW. Exhaust gas temperatures were found to reach a peak maximum of 560°C. Average full load steady state exhaust gas temperature varied with engine model and test schedule. Average exhaust gas compositions are summarized in Table 3.1:

<i>Exhaust Gas Composition with Entrained Air</i>	
O ₂	17.1 – 18.7%
CO ₂	2.8%
CO	20 – 60 ppm
NO _x	90 – 120 ppm (@15% O ₂ , dry)

<i>Exhaust Gas Composition without Entrained Air</i>	
O ₂	15.5 %
CO ₂	3.4 – 4.0%
CO	90 - 200 ppm
NO _x	88 - 96 ppm (@15% O ₂ , dry)

Table 3.1: Average Experimental Steady State Exhaust Gas Composition

3.2 Reactor Operating Conditions

The average recirculation reactor temperature was controlled at a range of 700 to 800°C, with a mean residence time inside the recirculation zone of 0.69 to 0.75 sec with entrainment and 1.1 to 1.38 sec without entrainment respectively. Since turbine exhaust has a maximum temperature of 560°C at full load, the exhaust gas temperature had to be increased by at least 140 -180°C. In these tests this was done by first raising the exhaust temperature to 620°C through the use of a duct burner. In the normal operation the duct burner was also used to burn up the entrained air to give the exhaust/air flow a composition similar to pure turbine exhaust as discussed previously.

The final desired temperature rise in the reactor (from 620°C to reactor temperature) was obtained via autoignition of auxiliary turbine fuel, injected into the hot turbine exhaust duct between turbine and reactor. The auxiliary fuel needed to increase the reactor temperature to 740 °C was observed to be 25 % of the turbine fuel consumption. At full load and maximum auxiliary fuel injection, steady state conditions were reached within minutes. With the decay of thermal transients, duct burner set point was decreased while the auxiliary fuel flow was held constant, thereby controlling the reactor temperature.

The reactor geometry (see Figure 2.3) allowed for 30 to 40% recirculation, a value determined with the water model. The steady state maximum pressure drop across the entire system, including duct, duct burner and reactor was found to be 6.5 inches of water or 1620 Pa at constant steady state intake air mass flow of 26 kg/s. Reactor chamber insulation reduced average reactor outside wall temperature to about 30°C.

The average reactor operating conditions are summarized in Tables 3.2 below:

<i>Reaction chamber</i>	<i>Without entrainment</i>	<i>With entrainment</i>
Pressure loss across entire system	840 Pa	1620 Pa
Mean final reactor temperature	700 – 780°C	700 – 780°C
Auxiliary fuel consumption	6 L/min	6 L/min
Residence time in recirculating zone	1.1 – 1.38 sec	0.69 – 0.75 sec

Gas composition (full load and air entrainment)		
	<i>before reactor</i>	<i>after reactor</i>
O ₂	17.1 – 18.7%	11.8 – 12.7%
CO ₂	2.8%	5.3 – 6.1%
CO	20 – 60 ppm	20 – 55 ppm (T > 700°C)
NO _x	90 – 120 ppm (@15% O ₂ , dry)	36 ppm (@15% O ₂ , dry)

Gas composition (full load and no air entrainment)		
	<i>before reactor</i>	<i>after reactor</i>
O ₂	15.5 %	11.5 – 12.4%
CO ₂	3.4 – 4.0%	6.0 – 6.2%
CO	90 - 200 ppm	60 – 150 ppm (T > 700°C)
NO _x	88 - 96 ppm (@15% O ₂ , dry)	21 ppm (@15% O ₂ , dry)

Tables 3.2: Average Experimental Conditions

At steady state operation, CO emissions were slightly reduced in the reactor from initial concentrations in the turbine exhaust (see Table 3.2). The level of CO reduction increases with increasing reactor temperature. At temperatures below 700°C an increase in CO due to incomplete auxiliary fuel combustion was observed.

It was found that measured NO_x emissions increased by approximately 10 ppm, when the reactor was brought to operating temperature. This increase appeared to be dependent on the amount of auxiliary fuel added and the corresponding average reactor temperature and independent of the initial NO_x level. It can therefore be reasoned, that the autoignition process of auxiliary fuel as well as the duct burner form NO_x in an overall lean combustion zone and increase the net NO_x concentration by 10 ppm.

Since additional combustion of fuel lowers the O₂ content, net NO_x measurements are adjusted to 15% O₂. Once modified by “numerical air addition or subtraction”, NO_x concentration were

found to decrease when burner is turned on and auxiliary fuel is injected. This observation indicates that amount of NO_x formed per mass fuel consumed, in the lean recirculation zone, is less than the amount of NO_x produced per mass fuel consumed in the gas turbine combustor. In other words, duct burner and auxiliary fuel combustion lower the O_2 content more effectively, than they increase the level of NO_x .

3.3 NO_x Removal with Cyanuric Acid (CYA)

3.3.1 NO_x Removal Data

Figure 3.2 shows recorded data from a typical experiment. In the figure dry NO_x concentrations are shown as measured, and as adjusted to 15% O_2 . These NO_x concentrations were obtained for four molar CYA/NO_x ratios and an average temperature of 750 C in the recirculating section of the reactor. NO_x concentrations were allowed to reach steady state before any CYA feed rate changes were made. It can be seen that NO_x removal increases with increasing CYA injection. NO_x reduction from an initial concentration of 96 ppm to as low as 21 ppm was achieved. Highest NO_x reduction occurred at a CYA/NO_x ratio of 1.15. This ratio is higher than observed for gaseous isocyanic acid (HNCO) injection [Perry, 1991]. If CYA decomposes to 3 HNCO molecules, a theoretical ratio of $\text{CYA}/\text{NO}_x = 1/3$ should be sufficient to achieve significant NO_x reduction.

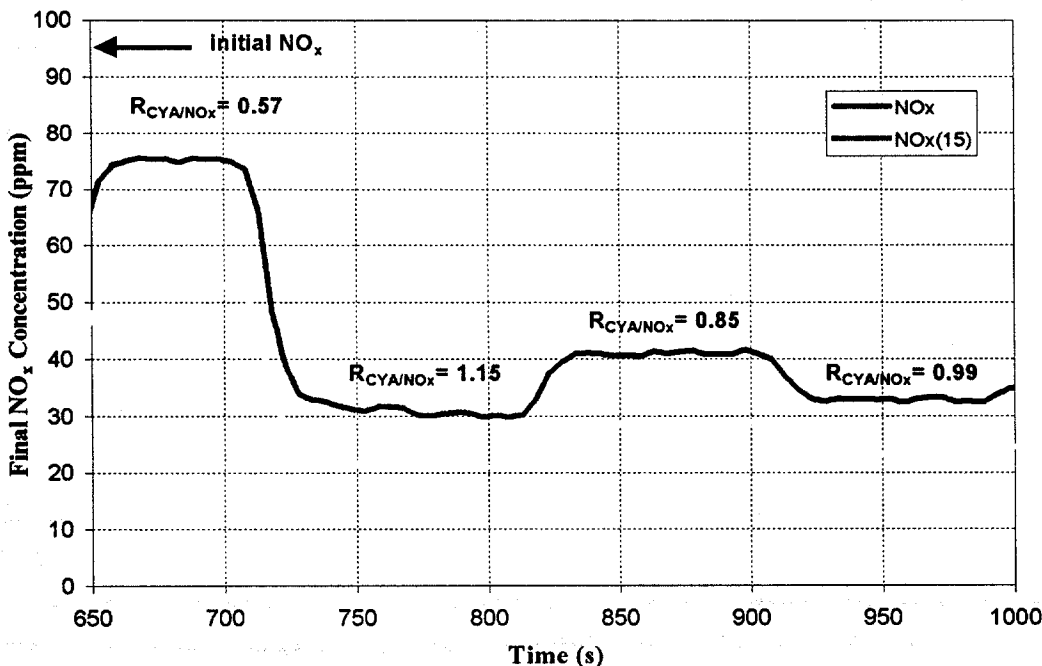


Figure 3.2: NO_x Concentration Data versus CYA/NO_x Ratio at fixed Average Reactor Temperature of 750°C.

The encountered high CYA/NO_x ratios might be explained by insufficient decomposition of the CYA ($(\text{HNCO})_3$) to the isocyanic acid monomer (HNCO). Since sublimation and cracking of the

reagent is dependent on the square of the particle diameter, CYA powder size distribution can have a significant impact on the process efficiency. If particle size is process limiting, smaller reagent particle size should result in decreased CYA/NO_x ratios. Compounding the effect is the used mode of CYA injection. The slurry water, which surrounds the injected CYA charge, has to evaporate before individual CYA particles can be heated to sublimation. The CYA decomposition process at very high temperatures, such as in a flame front leads to oxidation of HNCO and NO formation. (The higher ratio may also be due to the lower initial NO_x concentration utilized in these experiments.)

Injection location and residence time at elevated temperature can thus be crucial to the delivery of HNCO to the recirculation zone and thereby determine the efficiency of the overall process. Thus, injection close to the reactor results in incomplete decomposition to (HNCO)₃, while injection too close to the duct burner can cause a NO increase. This limitation as to the best location to inject the cyanuric acid was compounded by the fact that for the test with entrained air (most of the experiments) residual flame packets were observed to propagate the length of the duct limiting the effectiveness of the process for both reasons.

3.3.2 NO_x Removal from Exhaust with Entrained Air

Figure 3.3 shows the ratios of final and initial NO_x concentration at CYA/NO_x ratios of 0.48 to 1.13. The measured NO_x values were adjusted to 15% O₂ and compared to the average steady state NO_x concentration (also at 15% O₂). Data for each individual set of experimental parameters were similar to those seen in Figure 3.2. For three different engine types 37 to 50% NO_x reduction was achieved. The reactor temperatures ranged from 700°C to 780°C. The lowest reduction occurred at a temperature of 700°C and the highest reduction values were observed at an average temperature of 745°C. The different icons used represent different engine models. NO_x reduction appeared largely independent of CYA / NO_x ratio in the experimental range. Since entrained air required higher duct burner heat input, duct temperature distribution was found to be very inhomogeneous. Duct burner flame length reached a maximum of approximately 8m, limiting the region of auxiliary fuel and CYA injection. Auxiliary fuel was found to spontaneously ignite at the point of injection. This led to an unsteady diffusion controlled combustion process rather than the desired homogeneous, overall lean reacting flow. To prevent burning of the injected CYA in this hot combusting process, fuel injection was moved to the entrance of the reactor. The performance of the duct burner was slightly improved by changes in the flow geometry, yet flame lengths remained excessive keeping the temperature distribution nonhomogeneous. The resulting poor mixing and incomplete reagent decomposition can explain the relatively low level of NO_x reduction.

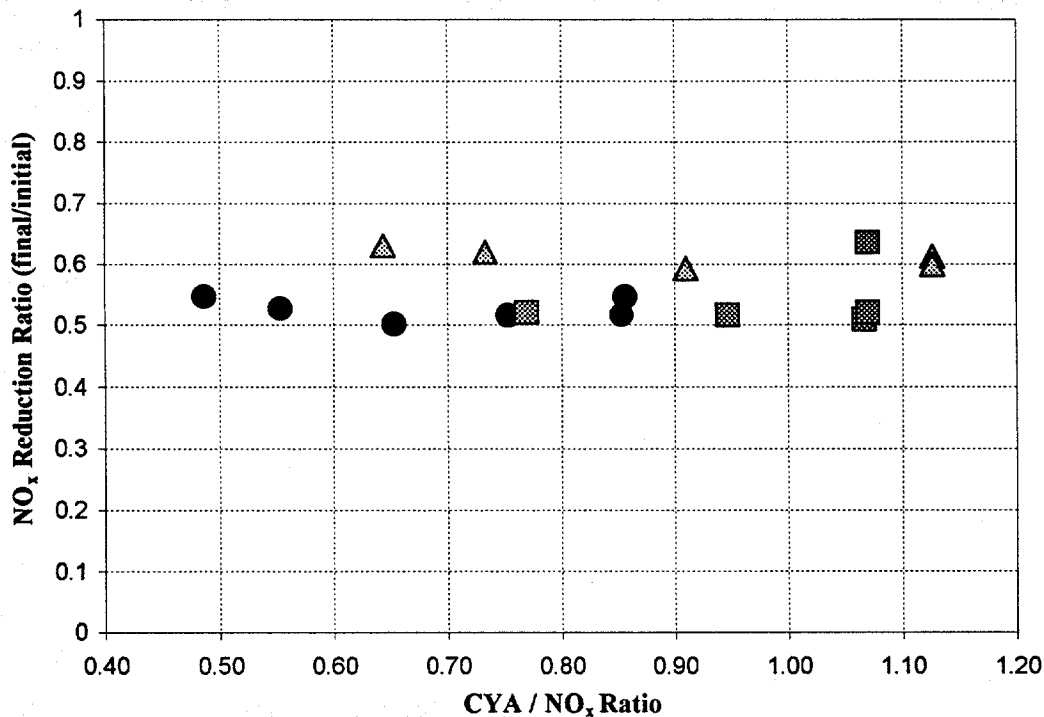


Figure 3.3: Ratio of Initial and Final NO_x Concentrations versus CYA/NO_x ratio. All NO_x measurements are adjusted to 15% O₂ content.

3.3.3 NO_x Removal from Exhaust without Entrained Air

Figure 3.4, 3.5 and 3.6 show final NO_x concentrations versus CYA/NO_x ratio. The reduced mass flow (without entrained air) increases the mean residence time inside of the reaction chamber and requires less heat input from the duct burner. The corresponding burner flame lengths were short (<1m), which allowed for injection of auxiliary fuel and CYA closer to the burner. Injection at a location closer to the burner increases residence time of CYA in the hot exhaust gases, improves mixing and resulted in a more efficient process.

Figure 3.4 shows the NO_x reduction achieved with injection of CYA and fuel in the same locations as used in the tests with air entrainment. NO_x reduction is therefore not optimized and ranges at about 50%. The marked data points illuminate the effect of injection location. Here 15% of the auxiliary fuel was injected 2 m further upstream while all other parameters remained the same. The initial NO_x concentration of 83 ppm was reduced to 30 ppm at a CYA/NO_x ratio of 1.12 and an average reactor temperature of 730°C. Throughout this test average reactor temperature ranged between 700 and 748°C.

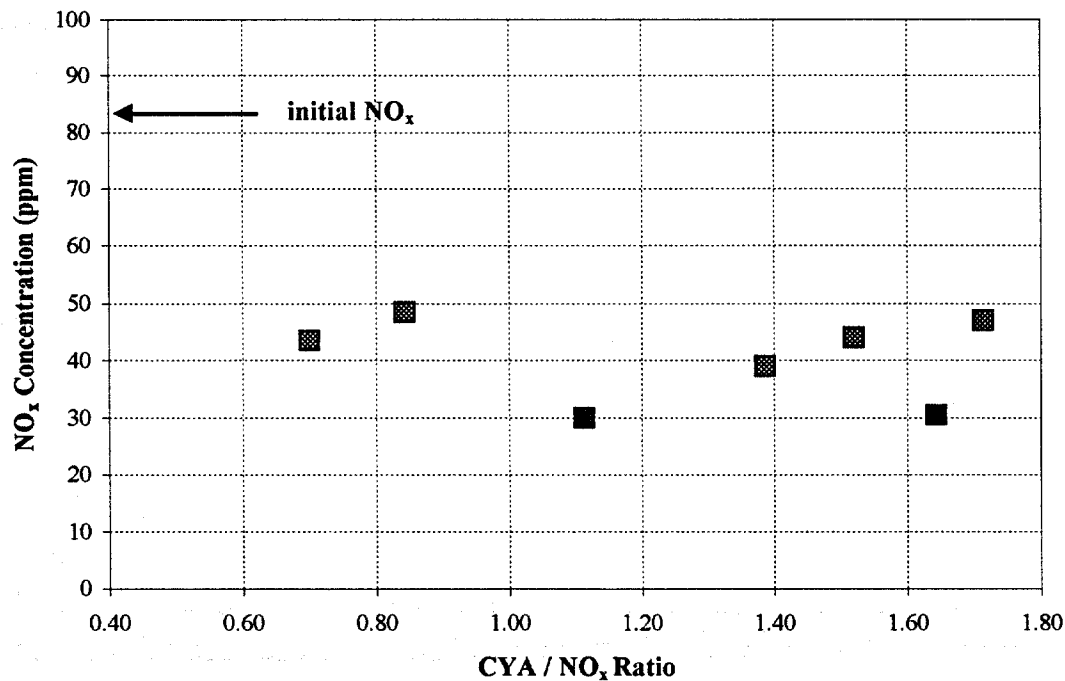


Figure 3.4: Final NO_x Concentrations versus CYA/NO_x ratio. All NO_x measurements are adjusted to 15% O₂ content. CYA and auxiliary fuel are injected at the same locations as in the previous tests with entrained air. The marked data points were obtained with a changed fuel injection location.

In Figure 3.5 CYA injection was moved to a location approximately 5 m down stream from the duct burner. The fuel was injected in the same location as during the tests with entrained air, at the reactor entrance. The resulting NO_x reduction improved significantly. Initial NO_x concentrations of 95 ppm were reduced to final values of 25.4, 31.6 and 27.6 ppm at CYA/NO_x ratios of 0.56, 0.70 and 0.71 respectively. The average reactor temperature ranged between 766 and 800°C. The increase in process efficiency indicated by the CYA/NO_x ratios is attributed to the change in injection location, resulting in a better utilization of the injected reagent.

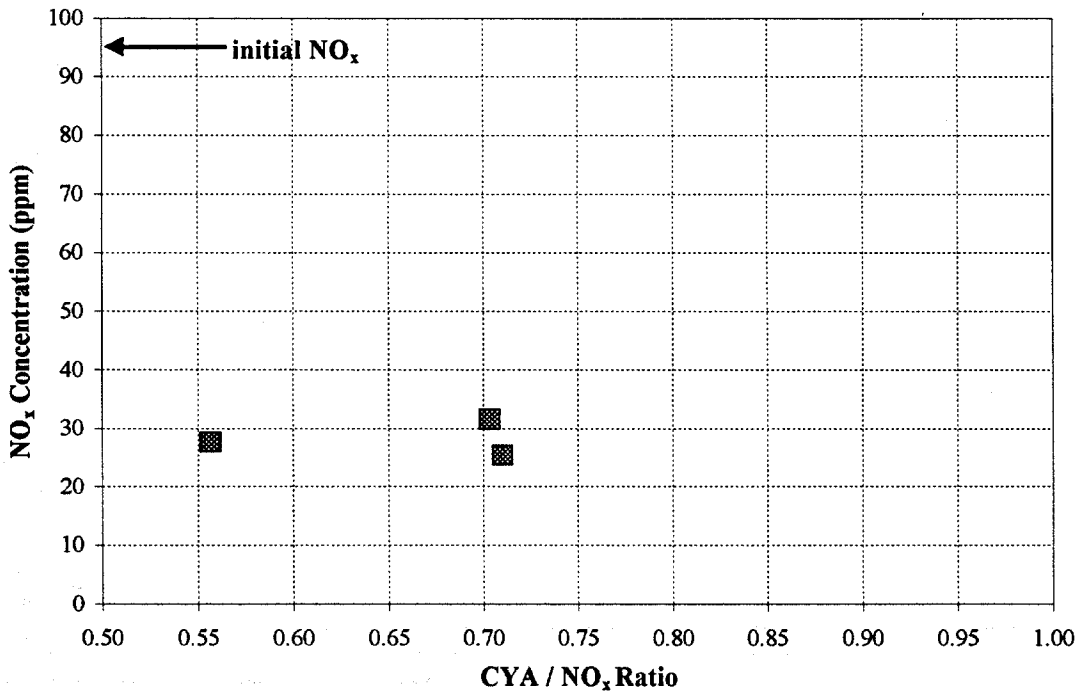


Figure 3.5: Final NO_x Concentrations versus CYA/NO_x ratio. All NO_x measurements are adjusted to 15% O₂ content. In this test the location of the CYA injection was moved closer to the reactor.

Combining both changes to auxiliary fuel and to CYA injection location led to the NO_x reduction results seen in Figure 3.6. At an average reactor temperature of 750°C throughout the test, a maximum reduction from the initial NO_x concentration of 96 ppm to a final NO_x concentration of 20.8 ppm was observed. The reduction process improved with increased CYA/NO_x ratio to find the maximum at a value of 1.15. This ratio is higher than those encountered in the previous Figure 3.5. Examining the temperature distribution in the duct show an average duct temperature of 620°C. In the previous test this temperature was 720°C due to mass flow and different engine test conditions. It can be reasoned that this higher average temperature accelerates the decomposition of CYA and therefore improves the reduction efficiency. This observation also indicates the importance of the performance of the duct burner. Careful control of the average duct temperature in combination with a homogeneous temperature profile allows further optimization of the positive synergism between fuel and CYA injection.

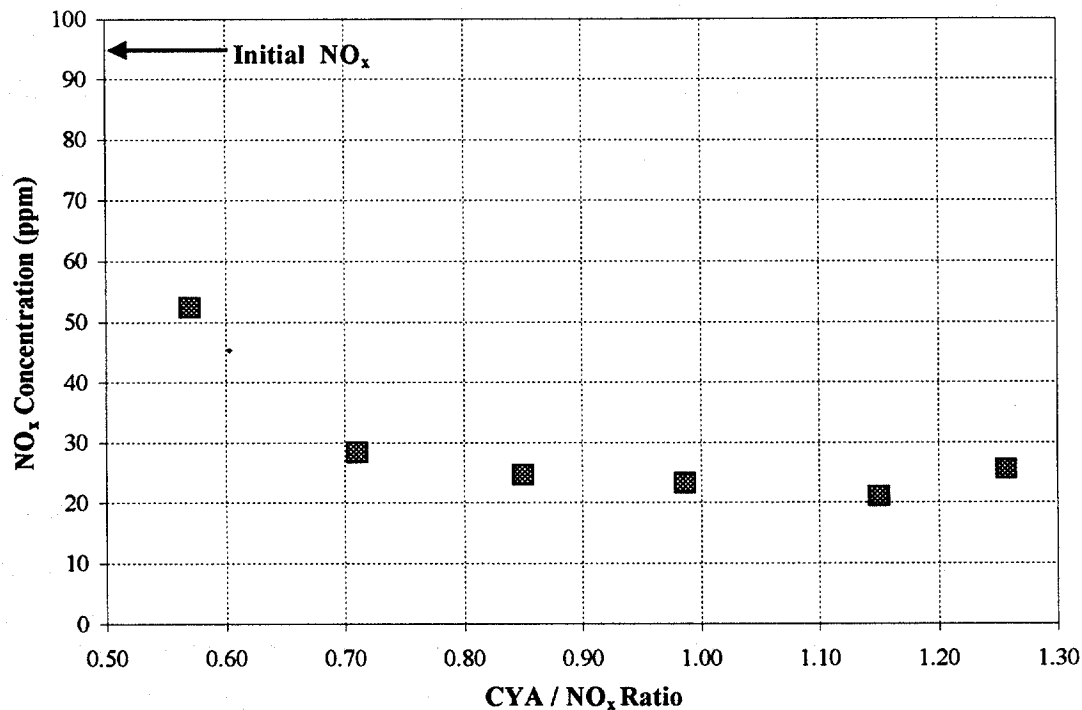


Figure 3.6: Ratio of Initial and Final NO_x Concentrations versus CYA/NO_x ratio. All NO_x measurements are adjusted to 15% O₂ content. CYA and auxiliary fuel injection location differed from previous tests.

4.0 TECHNICAL AND ECONOMIC SUMMARY

Based upon the results of this testing and on the projected cost associated with operation on a Allison 501KB5 (4MW class, 34lbs/sec) Gas Turbine a summary of the benefits and associated cost are listed below. The cost of operation assumes that the effective cost for cyanuric acid is \$0.27-0.35/lb and that 0.75-1.5gal/min of fuel is needed (with/without heat recovery unit). (Note that if the system is a combined cycle system with a use for the additional heat generated this would not be considered an additional cost.)

Successful application of the RAPRENOX process to a gas turbine would offer the following advantages:

- Reduction of approximately 84% of the NO_x in a typical exhaust system with affecting gas turbine operation. (21 ppm starting at 140 ppm.)
- Retrofittable with only exhaust modification needed i.e., no turbine modification, to allow for a reaction vessel installation.
- Reduction in CO and hydrocarbon concentrations possible due to inclusion of reaction vessel that makes secondary combustion part of the design.
- No slippage of ammonia or isocyanic acid observed.

- Is a cost effective means for reducing NO_x without the addition of a hazardous chemical, such as ammonia, or the major cost of a large SCR catalyst installation.

The cost estimate for the operation of the RAPRENOX system on a 4MW gas turbine is derived from the following.

- o Assumptions:
 - 4MW gas turbine using 380 gallons fuel/hr.
 - 27 lbs/hr NO_x measured as NO₂/hr
 - 90% NO_x removal efficiency
 - \$0.70/gallon for jet fuel
- o Cost Calculations
 - Using optimized system and assuming 2.7 lbs of cyanuric acid needed per pound of NO_x for maximum NO_x reduction
 - Capital cost is approximated by cost of existing delivery system and appropriate reactor.

Table 4.1: Estimate of Cost for Application of RAPRENOX to Gas Turbine Exhaust

<u>Estimate</u>	<u>High</u>	<u>Low</u>
Installed Cost (\$35/kW)	\$180,000	\$140,000
Annual Operating Cost @ 50% Annual Load Factor:		
Reagent Cost @ \$0.27/lb and 1.9lbs/lb		\$ 85,000
Reagent Cost @ \$0.35/lb and 2.5lbs/lb	\$145,000	
Additional Fuel @ 1.5gal/min of fuel input and \$0.70/gal.	\$272,000	
Additional Fuel @ 0.75gal/min of fuel input and \$0.70/gal.		\$138,000
	\$ 4,000	\$ 4,000
Other Operating and Maintenance @ 3% FCI		
Capital Charges @ 20%	\$ 36,000	\$ 28,000
Annual Total	\$457,000	\$255,000

In conclusion, the use of the RAPRENOX process for NO_x control provides a cost effective method for reducing NO_x emissions from gas turbines. The cost per ton of NO_x removed is between \$4300-\$7700. Note that in a combined cycle application this cost would come down even further to \$3140/ton of NO_x. The use of the technology for gas turbines that employ a heat recovery system would significantly reduce the operating cost of the technology and make it a clear choice for retrofit applications. It can also be used in other applications where the ability to follow load or provide NO_x reduction without the use of toxic ammonia is required.

5.0 FUTURE WORK:

Future work for this technology would include a redesign of the burner/duct system to provide a better test for following changing load conditions and for optimizing the location of the injection system. In addition more work at high load would be useful to better understand the role that low initial NO_x plays on the need for additional cyanuric acid injection (approximately 1-1 CYA-

NO_x) at initial NO_x less than 100 ppm. Also more testing on an engine run for extended hours of operation, something that could not be done at the test facility would be helpful.

6.0 References

Lovett, J.A., and Mick, W.J., "*Development of a Swirl and Bluff-Body Stabilized Burner for Low-NO_x Lean-Premixed Combustion*" ASME paper 95-GT-166, 1995

Perry, R.A., "*Application of RAPRENO_x to Diesel Emission Control*" Technology assessment and Research program for Offshore Minerals Operations, U.S. Department of the Interior Minerals Management Service, DOI No. 85K-SC293V, pp 185-190, 1991

Rhine, J.M., and Tucker R.J., "*Modelling of Gas-Fired Furnaces and Boilers*", British Gas, McGraw-Hill, ISBN 007 7073053, 1991

Streichsbier, M. "*Non-Catalytic NO_x Removal from Gas Turbine Exhaust with Cyanuric Acid in a Recirculating Reactor*" Dissertation, Department of Mechanical Engineering, University of California at Berkeley, 1998

Perry, R.A., "*Application of RAPRENO_x to NO_x Control in Diesel Generators*", First Int. on Combustion Technologies for a Clean Environment, Lisbon, Portugal, 1991

APPENDIX A

Alison Gas Turbines

	<u>501-KH</u>	<u>571-KA</u>
Shaft HP (kW)	5088(3800)	7925(5910)
Exhaust Temp F	1055	1067
Loss, inlet (" H2O)	4	4
Loss, outlet	10	
Specific Fuel Consumption		
Btu/shp-hr (MJ/kWh)	9129 (12915)*	7510(10625)
Fuel Flow lbs/hr (Max)	2275	2939
Air Flow lbs/sec (kg/sec)	33.8(15.36)	43.3(19.65)
Exhaust Flow lbs/sec	34.1(34.4*)	44.1*
Reference Fuel		
LHV, btu/lb btu/scf (kj/m3)	20420	904 (35,500)
Fuel Flow MMBTU/hr	46.449	60.016
Emissions Estimates:		
NOx 15%O2 dry, ppm	141	88
CO 15% O2 dry, ppm	24	30
CO2 %	3.29	3.36
O2 %	13.65	13.50
NOx lbs/eng-hr	27.1	21.7

* Calculated from data available.